Differential regulation of the retinoblastoma family of proteins during cell proliferation and differentiation

Judit GARRIGA*, Ana LIMÓN*, Xavier MAYOL*[1], Sushil G. RANE*, Jeffrey H. ALBRECHT†, E. Premkumar REDDY*, Vicente ANDRÉS‡ and Xavier GRAÑA*[2]

*Fels Institute for Cancer Research and Molecular Biology and Department of Biochemistry, Temple University School of Medicine, 3307 North Broad Street, Philadelphia, PA 19140, U.S.A., †Department of Medicine, Hennepin County Medical Center, 701 Park Avenue, Minneapolis, MN 55415, U.S.A., and ‡Division of Cardiovascular Research, St. Elizabeth's Medical Center, 736 Cambridge Street, Boston, MA 02135, U.S.A.

In the present study we have analysed the regulation of pocket protein expression and post-transcriptional modifications on cell proliferation and differentiation, both *in vivo* and *in vitro*. There are marked changes in pocket protein levels during these transitions, the most striking differences being observed between p130 and p107. The mechanisms responsible for regulating pocket protein levels seem to be dependent on both cell type and pocket protein, in addition to their dependence on the cell growth status. Changes in retinoblastoma protein and p107 levels are independent of their state of phosphorylation. However, whereas p130 phosphorylation to forms characteristic of quiescent/differentiated cells results in the accumulation of p130 protein, phosphorylation of p130 to one or more forms characteristic of cycling cells is accompanied by down-regulation of its protein levels. We also show here that the phosphorylation status and protein levels of p130 and p107 are regulated *in vivo* as in cultured cells. *In vivo*, changes in p130 forms are correlated with changes in E2F complexes. Moreover, the modulation of p130 and p107 status during cell differentiation *in vitro* is consistent with the patterns of protein expression and phosphorylation status found in mouse tissues. Thus in addition to the direct disruption of pocket protein/E2F complexes induced by cyclin/cyclin-dependent kinase, the results we report here indicate that the differential modulation of pocket protein levels constitutes a major mechanism that regulates the pool of each pocket protein that is accessible to E2F and/or other transcription factors.

INTRODUCTION

The retinoblastoma family of pocket proteins, which comprises retinoblastoma protein (pRB), p107 and p130, is believed to have crucial roles in processes of cell proliferation and differentiation [1–3]. Pocket protein function is associated with the regulation of transcription factors belonging to the E2F family, which are necessary for cell cycle progression. Pocket proteins form complexes with E2Fs and repress the transcription of genes required for cell cycle progression that contain E2F sites in their promoters. It is widely accepted that the state of phosphorylation of pocket proteins is responsible for regulating their interaction with E2F proteins, and the phosphorylation of pocket proteins is regulated in response to both positive and negative growth signals. These signals converge on the family of cyclin/cyclin-dependent kinase (CDK) holoenzymes, which are sequentially activated throughout the cell cycle. Hyperphosphorylation of pocket proteins by cyclin/CDKs in mid-G_1 results in the disruption of pocket protein/E2F complexes and the transcription of E2F-dependent genes necessary for cell cycle progression [1–3]. Therefore the availability of active cyclin/CDKs determines the amount of hypophosphorylated forms of each pocket protein able to associate with E2F in proliferating cells. In non-proliferating cells, G_1/S cyclin/CDK holoenzymes are not active and pocket proteins can therefore associate with E2Fs.

Each pocket protein has a preference for forming complexes with specific E2F members at specific stages of the cell cycle. The formation of specific pocket protein/E2F complexes is regulated, at least in part, by the availability of specific E2F members. Thus, whereas E2F-4 is characteristic of quiescent cells, E2F-1, E2F-2 and E2F-3 are primarily transcribed from mid-G_1 [1,2]. Several reports suggest strongly that p130/E2F complexes have a role during G_0 and in very early stages of the G_1 phase. p130 is the major pocket protein associated with E2F species in quiescent cells such as human and rodent fibroblasts [4–8], human T lymphocytes [9,10], terminally differentiated muscle cells [11–14], neuronal PC19 cells [13] and melanocytes [15]. The E2F partner of p130 has consistently been identified as E2F-4 in the above-mentioned studies. Furthermore p130 accumulates and is phosphorylated to specific forms that bind to E2F-4 when cells exit from the cell cycle to quiescence [16]. p130/E2F complexes accumulate when cells exit from the cell cycle, but are scarce when cycling cells enter G_1 from mitosis, suggesting that these complexes perform their major role in quiescent cells rather than during G_1 [6,16].

Although pRB has also been reported to form complexes with E2F in differentiating cells [4], pRB seems to bind preferentially to E2F in mid–late G_1 and S phases. Similarly, p107 forms complexes with E2F predominantly in late G_1 and S phases, with E2F-4 as its primary E2F partner. Transcription of the E2F-1

Abbreviations used: CDK, cyclin-dependent kinase; DMEM, Dulbecco's modified Eagle's medium; EMSA, electromobility shift assay; FBS, fetal bovine serum; G-CSF, granulocyte colony-stimulating factor; IL-3, interleukin 3; PH, partial hepatectomy; pRB, retinoblastoma protein; VSMCs, vascular smooth-muscle cells.

[1] Present address: Unitat de Biologia Cellular i Molecular, Institut Municipal d'Investigació Medica (IMIM), Dr. Aiguader 80, 08003 Barcelona, Spain.
[2] To whom correspondence should be addressed (e-mail xavier@sgi1.fels.temple.edu).

gene is under E2F-dependent negative control in G_0 and early G_1, coinciding with the presence of p130/E2F-4 complexes, which are found only before cyclin/CDK activation in mid-G_1 but not at later stages of the cell cycle [6,7,16]. Disruption of p130/E2F-4 complexes on cyclin/CDK activation in mid-G_1 is typically followed by formation of pRB/E2F-1 and p107/E2F-4 complexes, although in certain cell types pRB/E2F-4 complexes are also found [4,10]. In contrast with p130/E2F complexes, E2F complexes containing pRB and p107 are detected during late G_1 and S phases. It has therefore been suggested that phosphorylation of pRB and p107 by cyclin/CDK is modulated in a manner so that hyperphosphorylated and hypophosphorylated forms are kept in balance and any required pool of hypophosphorylated pRB or p107 able to interact with E2F will be maintained during mid–late G_1 and S phases [1], thus allowing the accurate differential transcriptional regulation of E2F-dependent genes.

Although cyclin/CDK phosphorylation of pocket proteins seems to be critical in regulating their interaction with E2F proteins, the complex array of pocket protein/E2F interactions observed during the cell cycle and cell cycle exit indicates that there must be further mechanisms of pocket protein regulation in addition to cyclin/CDK phosphorylation. Changes in p130 and p107 levels have been occasionally correlated with changes in the composition of E2F complexes in certain models [14]. Nevertheless regulation of pocket protein levels has rarely been considered as a major mechanism controlling the activity of pocket proteins. In the present study we have investigated this possibility by analysing the pocket protein status in several models of cell proliferation and differentiation. Our results, both *in vitro* and *in vivo*, indicate that pocket protein levels are differently regulated during these processes and suggest that phosphorylation and dephosphorylation events are co-ordinated with modulation of pocket protein levels to regulate the amount of each pocket protein available to associate with and repress E2F and other cellular proteins at particular cellular stages.

EXPERIMENTAL

Cell cultures and tissues

T98G human glioblastoma cells and NIH-3T3 mouse fibroblasts were grown in Dulbecco's modified Eagle's medium (DMEM) plus 10% (v/v) fetal bovine serum (FBS) supplemented with penicillin/streptomycin. NIH-3T3 and T98G cells were synchronized as described previously [16,17]. Asynchronously growing T98G cells were used as a control for the identification of the different phosphorylated forms of pocket proteins in all Western blot analyses. Skeletal muscle L6 (rat) and C2C12 (mice) cell lines were grown as myoblasts in DMEM plus 20% (v/v) FBS supplemented with penicillin/streptomycin until they reached 60–70% confluence. At that point, FBS was switched to 2% (v/v) horse serum to induce differentiation. NFB cells, which are derived from a clone of C2 cells and do not differentiate [18], were grown similarly to C2C12 cells but after being switched to 2% horse serum they became quiescent. The murine interleukin 3 (IL-3)-dependent 32Dcl3 cell line was maintained in RPMI 1640 medium supplemented with 10% FBS and 10% (v/v) WEHI3B-conditioned medium as a source of crude IL-3 [19]. For induction of differentiation, cells were centrifuged down and resuspended in a medium containing 10% FBS and 15% (v/v) CHO-conditioned medium as a source of granulocyte colony-stimulating factor (G-CSF) [19]. On each of the following days, smears were prepared from an aliquot of cell culture with a Cytospin and were stained with May–Grunwald/Giemsa for morphological analysis [19]. Primary vascular smooth-muscle cells (VSMCs) were isolated essentially as described [20]. Primary VSMCs and rat aorta A10 cells were maintained in DMEM supplemented with 10% and with 20% fetal calf serum respectively (growth medium). To render cells quiescent, cultures were maintained for 3 days in DMEM supplemented with 0.5% fetal calf serum. Quiescent primary VSMCs were serum re-stimulated with growth medium. Protein extracts of VSMCs [21] and A10 cells [22] were prepared as described previously.

Mouse tissues were all obtained from the same animal sacrificed by cervical dislocation. Tissues were dissected and immediately frozen in liquid nitrogen and kept at −80 °C until use. Tissue extracts were prepared in lysis buffer [50 mM Tris/HCl (pH 7.4)/0.1% (v/v) Triton X-100/5 mM EDTA/250 mM NaCl/50 mM NaF/0.1 mM Na_3VO_4/1 mM PMSF/10 μg/ml leupeptin] with the aid of a tissue homogenizer (Polytron).

Electromobility shift assays (EMSAs)

EMSAs were performed by mixing either 8 μg of whole cell or 4 μg of nuclear protein extracts with 0.25 ng of γ-^{32}P-end-labelled double-stranded oligonucleotide probe containing the E2F-binding site of the E2 promoter in a total volume of 25 μl, as described previously [23]. Where indicated, 4 μl of the specific antibody were added. The sequences of the E2F oligonucleotides used were 5′-ATTTAAGTTTCGCGCCCTTTCTCAA-3′ (wild-type) and 5′-ATTTAAGTTTCGATCCCTTTCTCAA-3′ (mutant). T98G whole-cell extracts for EMSA were prepared in 5 × extraction buffer [100 mM Hepes (pH 7.4)/500 mM KCl/5 mM $MgCl_2$/0.5 mM EDTA/35% (v/v) glycerol/5 mM NaF/1 mM dithiothreitol/100 μg/ml PMSF/5 μg/ml aprotinin/5 μg/ml leupeptin] as described previously [23]. Nuclei from liver were obtained as described [24]. Nuclear extracts were obtained by disrupting the nuclei by sonication in 150 μl of the 5 × extraction buffer (see above).

Rat and mouse 70% partial hepatectomy (PH)

Partial (70%) hepatectomy was performed on 8-week–old male Sprague–Dawley rats and BALB/c mice as described previously [25]. At the indicated time points, animals were killed and the remnant liver tissue was harvested and flash-frozen in liquid nitrogen.

Rat model of balloon injury

Acute endothelial denudation of the left common carotid artery was performed essentially as described previously [26]. The right uninjured carotid artery was used as control tissue. At the indicated times after injury, rats were killed with sodium pentobarbital (intraperitoneal injection, 100 mg/kg of body weight), and both injured and uninjured common arteries were perfused with saline and dissected free of surrounding tissue. Arteries were frozen quickly in liquid nitrogen and stored at −80 °C until the preparation of the protein lysates as described previously [21]. Preparation of arteries and immunostaining for smooth-muscle α-actin was performed as described previously [21].

Western blots and immunoprecipitation

Protein extracts of cells were prepared in lysis buffer (see above) as described previously [27], with the exception of 32Dcl3 (see below). The protein content of tissue and cell lysates was measured by the method of Bradford (Bio-Rad) and 30–40 μg of protein per sample was loaded on to SDS/PAGE gels (Protogel; National Diagnostics). Crude cell extracts from 32Dcl3 cells were obtained by resuspending 10^7 cells in denaturing lysis buffer

[33.3 mM glucose/33.3 mM Tris/HCl (pH 7.4)/6.66 mM EDTA/2 M urea/2% (v/v) 2-mercaptoethanol/1% (w/v) SDS/0.001% Bromophenol Blue/0.66 mM PMSF/2 mM Na_3VO_4/4 μg/ml aprotinin/4 μg/ml leupeptin/4 μg/ml pepstatin]. After sonication, extracts were incubated at 65 °C for 15 min and quantified by absorbance at 260 and 280 nm. Polyacrylamide gels (6%, w/v) were used to analyse pRB-related proteins and 10% (w/v) polyacrylamide gels to detect the levels of the different cyclins. Proteins were transferred to PVDF membranes and immunoblotted with specific antibodies [27]. p107 patterns in carotid samples were determined by immunoprecipitation followed by Western blotting [27].

The antibodies used in these experiments were anti-p130 (SC-317), anti-p107 (SC-318), anti-pRB (SC-50), and anti-cyclin D3 (SC-182) rabbit polyclonal antibodies and anti-cyclin D1 (SC-246) mouse monoclonal antibody from Santa Cruz Biotechnology. Anti-pRB mouse monoclonal antibody (no. 14001A) was from Pharmingen. Anti-cyclin A rabbit polyclonal antibody was a gift from Dr. Pines and anti-cyclin E rabbit polyclonal antibody was a gift from Dr. Koff.

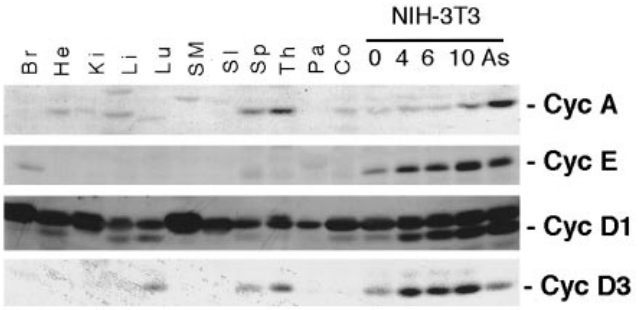

Figure 2 Expression of G1/S cyclins *in vivo* in adult mouse tissues

Protein extract (40 μg) obtained from the indicated mouse tissues was resolved by SDS/PAGE [10% (w/v) gel] and analysed by Western blotting as in Figure 1 by using specific antibodies as indicated at the right [top panel, cyclin A; second panel, cyclin E; third panel, cyclin D1 (indicated faster mobility band); bottom panel, cyclin D3]. NIH-3T3 cells at different stages of the cell cycle were used as a control for expression of cyclins (time points in hours after re-stimulation are indicated at the top). Lane As, asynchronous cells. Tissues are indicated at the top as in Figure 1.

RESULTS

Pocket protein levels and phosphorylation status in mouse tissues

The effects of pocket proteins on cell growth are dependent on cell type and several lines of evidence indicate that pocket proteins fulfil an important role in the differentiation of certain tissues [1,2]. We therefore sought first to compare the patterns of pocket protein levels and phosphorylation status *in vivo* by Western blotting in adult mouse tissues to ascertain whether there is any specificity in their tissue distribution. Figure 1 shows that the abundance of each pocket protein was highly variable between the different tissues studied. The highest levels of each pocket protein were detected in lung, spleen, thymus, and colon. However, whereas p130 was still abundant in brain, liver, pancreas, rectum and stomach, the levels of pRB and p107 in these latter organs were comparatively low or even undetectable, most notably regarding p107. With the exception of spleen and thymus, the state of phosphorylation of pocket proteins is characterized by the presence of underphosphorylated forms, which are characteristic of non-proliferating cells. In particular, p130 phosphorylated forms 1 and 2, characteristic of exit from the cell cycle in cultured cell lines [16,17], are also detected in adult tissues. These patterns are obviously reflecting that most of the cells in most adult tissues are non-dividing, differentiated cells. Because there is increasing evidence that p130 function is involved in processes of cell cycle exit and differentiation (see above), the high abundance of p130, particularly p130 forms 1 and 2, is consistent with the notion that it has a role in adult differentiated tissues.

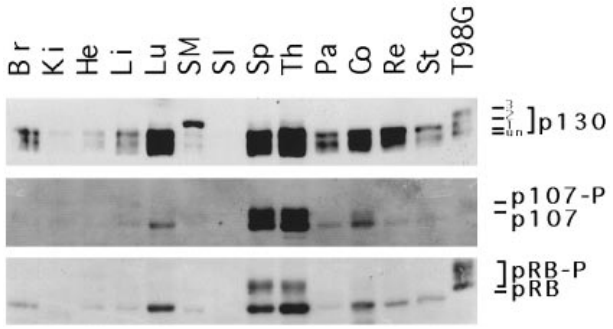

Figure 1 Patterns of expression and phosphorylation of p130, p107 and pRB *in vivo* in adult mouse tissues

Protein extract (40 μg) obtained from the indicated mouse tissues was resolved by SDS/PAGE [6% (w/v) gel]. Proteins were transferred to PVDF membranes and immunoblotted with specific antibodies (top panel, p130; middle panel, p107; bottom panel, pRB). Asynchronously growing T98G glioblastoma cells were used as a control for identification of the different phosphorylated forms of each pRB-family member (right-hand lane). Forms of each pocket protein are indicated at the right (un, unphosphorylated p130). Tissues are indicated at the top as follows: Br, brain; Ki, kidney; He, heart; Li, liver; Lu, lung; SM, skeletal muscle; SI, small intestine; Sp, spleen; Th, thymus; Pa, pancreas; Co, colon; Re, rectum; St, stomach. A non-specific band co-migrating with p130 form 3 was detected by the affinity-purified anti-p130 antibodies in skeletal muscle tissue extracts by Western blot analysis. This cross-reacting protein, in contrast with all p130 forms detected by Western blotting [16,17], was not immunoprecipitated by anti-p130 antibodies (results not shown) and probably corresponds to a highly abundant protein present in skeletal muscle tissue.

Spleen, thymus and colon are known to have a high cell renewal rate and therefore contain a significant number of cells progressing through the cell cycle [28]. This is consistent with the pattern of phosphorylated forms shown in Figure 1: both hyperphosphorylated pRB and p107 are present. Interestingly, very low levels of p130 form 3 (compared with the high levels of p130 forms 1 and 2) are detected in these tissues where hyperphosphorylated forms of pRB and p107 account for an important portion of total pRB and p107 proteins respectively (Figure 1; compare lanes Sp and Th). We have previously shown that when quiescent cells enter the cell cycle and progress through G_1, p130 is phosphorylated to form 3 and this is followed by down-regulation of p130 protein levels [16,17]. It is therefore conceivable that apart from abrogating p130/E2F interaction [16], phosphorylation to p130 form 3 triggers its down-regulation. Because even in the tissues with high cell renewal most of the cells are in G_0, and therefore contain p130 forms 1 and 2, it would be expected that very low levels of p130 form 3, if any, contributed by the cycling cells would be detected.

Because G_1/S cyclin/CDK holoenzymes are most probably the kinase activities phosphorylating pocket proteins during progression through the cell cycle, we analysed the expression of cyclins in mouse tissues to ascertain whether their expression is consistent with the detection of low levels of p130 form 3 and hyperphosphorylated pRB and p107 (Figure 2). Western blot analysis was performed with the same protein extracts as used for Figure 1. The expression of these proteins was also analysed in

protein lysates of NIH-3T3 cells progressing synchronously through G_1 as controls. As expected, expression of cyclins E and A was detected only in tissues of high cell renewal, spleen and thymus, where hyperphosphorylated pocket proteins were also present. In contrast, expression of cyclin D1 and D3 was also detected in tissues in which hyperphosphorylated forms of pocket proteins were not detected. Furthermore it is important to note that the presence of p130 forms 1 and 2 did not seem to be correlated with the expression of any particular cyclin.

Regulation of pocket proteins during differentiation

p130 seems to be the major pocket protein in E2F complexes during various differentiation programmes [11–15]. Our present results show that p130 forms 1 and 2 are the major forms of p130 in all adult mouse tissues analysed. Moreover, p130 is relatively abundant in some tissues in which the levels of pRB and p107 are low when compared to their respective levels in other tissues (Figure 1; compare, for instance, rectum and colon). Because many of these tissues are composed mostly of differentiated cells, these results suggest that there is differential regulation between pocket proteins in processes of cell differentiation. To evaluate such differences, we sought to analyse in detail two well-characterized models of cell differentiation *in vitro*: differentiation of mouse and rat myoblasts into myotubes and differentiation of mouse myeloid precursors along the granulocyte lineage.

Skeletal muscle differentiation *in vitro*

Studies on skeletal muscle cell lines have shown that, whereas undifferentiated myoblasts mostly contain p107/E2F complexes, and to a minor extent p130/E2F complexes, differentiation into myotubes results in the primary presence of p130/E2F complexes [11–14]. It has also been suggested that changes in p130 and p107 levels were involved in the formation of these E2F complexes [14]. Therefore we sought to analyse in detail the patterns of expression and phosphorylation of p130 and p107 proteins during skeletal muscle cell differentiation of rat L6 and mouse C2C12 cells by Western blotting.

Both L6 and C2C12 proliferating myoblasts contained a pattern of p130 forms (unphosphorylated protein and phosphorylated forms 1, 2 and 3) similar to the pattern of phosphorylation of exponentially growing, asynchronous glioblastoma human T98G cells (compare lane 0 of Figure 3 with lane T98G in Figure 1). However, placing either cell line in differentiation medium resulted in the rapid disappearance of p130 form 3 and a striking increase in the levels of phosphorylated p130 forms 1 and 2. This is in contrast with previous studies, which did not detect the appearance of these phosphorylated forms of p130 probably because of technical differences in the analysis. In contrast, p107 was present at high levels in proliferating myoblasts as both hyperphosphorylated and hypophosphorylated forms, its levels dropped markedly as a result of the differentiating transition, which is in agreement with the results reported by Kiess et al. [14] with L6 cells. Because p107/E2F complexes are not found in differentiated myotubes (see [11,13,14]), hypophosphorylation of p107 induced by cell cycle exit does not imply the formation of p107/E2F complexes, but rather the decrease in p107 levels observed in Figure 3 seems to prevent the formation of these complexes. In contrast, the increase in the protein levels of p130 forms 1 and 2, which are the only phosphorylated forms of p130 that bind to E2F-4 *in vivo* [16], is an event that might explain the abundance of p130/E2F observed in differentiated myotubes (see [11–14]). In conclusion, opposite changes in levels of p130 and p107 are correlated in a subtle manner with the changes in the composition of E2F complexes reported earlier, and this differential regulation might be sufficient to account for the composition of these pocket protein/E2F complexes.

Interestingly, levels of p107 decrease during the differentiation process in an independent manner with respect to its state of phosphorylation: hyperphosphorylated and hypophosphorylated p107 are down-regulated to the same extent, this effect being more apparent in L6 cells (Figure 3B). However, up-regulation of p130 protein levels during skeletal muscle myogenesis takes place exclusively in p130 forms 1 and 2 in both cell lines, suggesting that the phosphorylation state of p130 is related to the regulation of its protein levels (see the Discussion section). In this respect it is interesting to note that the kinase activities responsible for phosphorylating p130 to forms 1 and 2 are active in muscle cells that are irreversibly exiting from the cell cycle to terminal differentiation.

It has been shown previously that cell cycle withdrawal precedes phenotypic differentiation and cell fusion of C2C12 cells [29]. We therefore next sought to examine whether the regulation of phosphorylation of p130 during skeletal myogenesis is associated with exit from the cell cycle or with differentiation. To this end we used a differentiation-deficient variant of C2 cells, NFB cells, which were obtained after mutagenesis of C2 cells and selection for defective differentiation [18]. NFB and C2C12 proliferating myoblasts were harvested at different time points after placing them in differentiation medium (Figure 3C) and p130 patterns were analysed by Western blotting. As shown in Figure 3(D), the patterns of phosphorylation of p130 in quiescent undifferentiated NFB cells and quiescent C2C12 differentiated myotubes (Figure 3C) were indistinguishable after 1 day of incubation in differentiation medium. These results indicate that accumulation of p130 forms 1 and 2 occurs during exit from the cell cycle before differentiation and fusion of skeletal myoblasts.

G-CSF-mediated granulocytic differentiation of 32Dcl3 cells

32Dcl3 cells are non-tumorigenic diploid cells derived from normal mouse bone marrow that are dependent on IL-3 for growth and survival. G-CSF stimulates the terminal differentiation of 32Dcl3 cells into neutrophilic granulocytes [19,30]. When 32Dcl3 cells were placed in G-CSF-containing medium, they proliferated for the first 4–6 days and then exited from the cell cycle simultaneously with the appearance of mature forms of the granulocytic lineage (Figure 4A). By days 9–14, the entire population of cells was terminally differentiated to metamyelocytes and granulocytes (Figure 4A) [19].

32Dcl3 cells were induced to differentiate in the presence of G-CSF and processed for Western blotting and flow cytometric analysis and May–Grunwald/Giemsa staining. Figure 4(B) shows that p130 was consistently present as a mixture of phosphorylated forms resembling the patterns of some cells growing asynchronously during the proliferative phase (lanes 12 h to 2 d). By day 4, p130 form 3 was progressively replaced by form 2 and form 1 (Figure 4B, lane 4). p130 forms 1 and 2 accumulated between days 4 and 8 concomitantly with the arrest of cells with a G_1 DNA content and with the appearance of cells at different stages of granulocytic differentiation, including myelocytes, metamyelocytes and few mature granulocytes (Figures 4A and 4B). pRB was present in its hypophosphorylated and hyperphosphorylated forms during the proliferation phase; the hyperphosphorylated forms disappeared at the same time as cell cycle exiting and the accumulation of p130 forms 1 and 2 (Figure 4B). In contrast, hyperphosphorylated p107 was the major form of p107 during the proliferative phase, and its levels

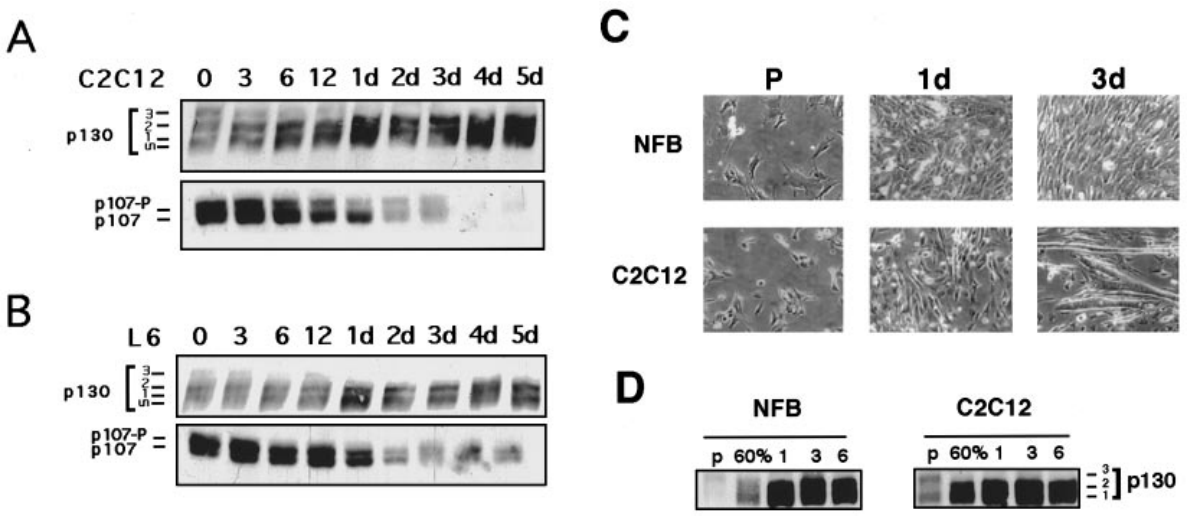

Figure 3 Changes in the phosphorylation status and levels of p130 and p107 during cell cycle exit and myogenesis in skeletal muscle

Skeletal muscle L6 (rat) and C2C12 (mouse) cells were grown as myoblasts until they reached 60–70% confluence. At that point, induction of differentiation resulted in the fusion of cells to form multinucleated myotubes (see the Experimental section). NFB cells, which are derived from a clone of C2 cells, became quiescent after exiting from the cell cycle, but were unable to differentiate (see the text). Protein extract (30 μg) obtained from C2C12 (**A**) or L6 (**B**) cells harvested at different time points after induction of differentiation was resolved by SDS/PAGE [6% (w/v) gel] and immunoblotted with specific antibodies (upper panel, p130; lower panel, p107) as in Figure 1. The different forms of each pocket protein are indicated at the left. (**C**) Comparison of the morphological changes induced in NFB and C2C12 cells by placing them in differentiation medium. C2C12 and NFB cells growing exponentially (labelled P) show the same morphology, but once they are induced to exit from the cell cycle C2C12 cells differentiate to myotubes, whereas NFB cells become quiescent but do not differentiate into myotubes (days in the differentiation medium are indicated). (**D**) Protein extract (30 μg) obtained from NFB or C2C12 cells growing exponentially (first lane), at 60% confluence (second lane) and at 1, 3 or 6 days after the cells were placed in differentiation medium, was resolved as in (**A**) and immunoblotted with anti-p130 antibodies.

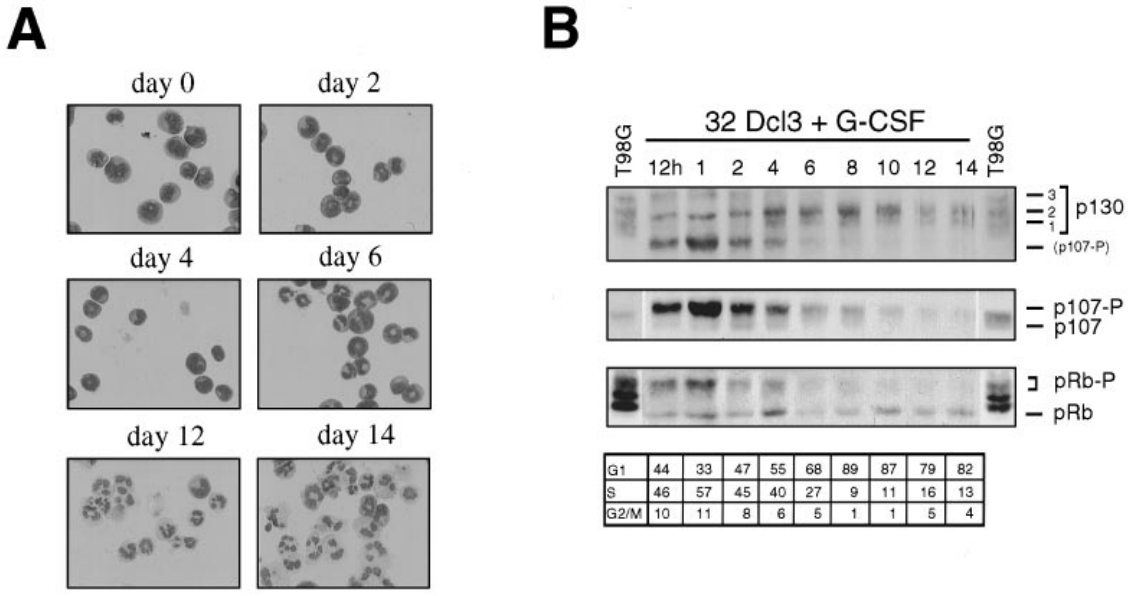

Figure 4 Changes in phosphorylation patterns and protein levels of p130, p107 and pRb during myeloid differentiation

(**A**) May–Grunwald/Giemsa staining of 32Dcl3 cells undergoing G-CSF-mediated differentiation. (**B**) Protein extract (60 μg) obtained from G-CSF-treated 32Dcl3 cells at different time points of granulocytic differentiation (see the Experimental section) was resolved by SDS/PAGE [6% (w/v) gel] and immunoblotted as in Figure 1 (top panel, p130; middle panel, p107; bottom panel, pRb). Asynchronously growing T98G glioblastoma cells were used as a control for the identification of different forms of pRb-family proteins (left-hand and right-hand lanes). Forms of each pocket protein are indicated at the right. The percentage of cells at each phase of the cell cycle is indicated at the bottom. The lot of affinity-purified anti-p130 antibodies used in this Western blot cross-reacted with p107, as indicated in the p130 panel.

decreased markedly by day 4 without significant accumulation of hypophosphorylated p107. In conclusion, pocket protein levels are again shown to be differentially regulated during cell differentiation. The pattern of p130 protein levels and the presence of p130 phosphorylated forms 1 and 2 are consistent with a role for p130 during this differentiation process.

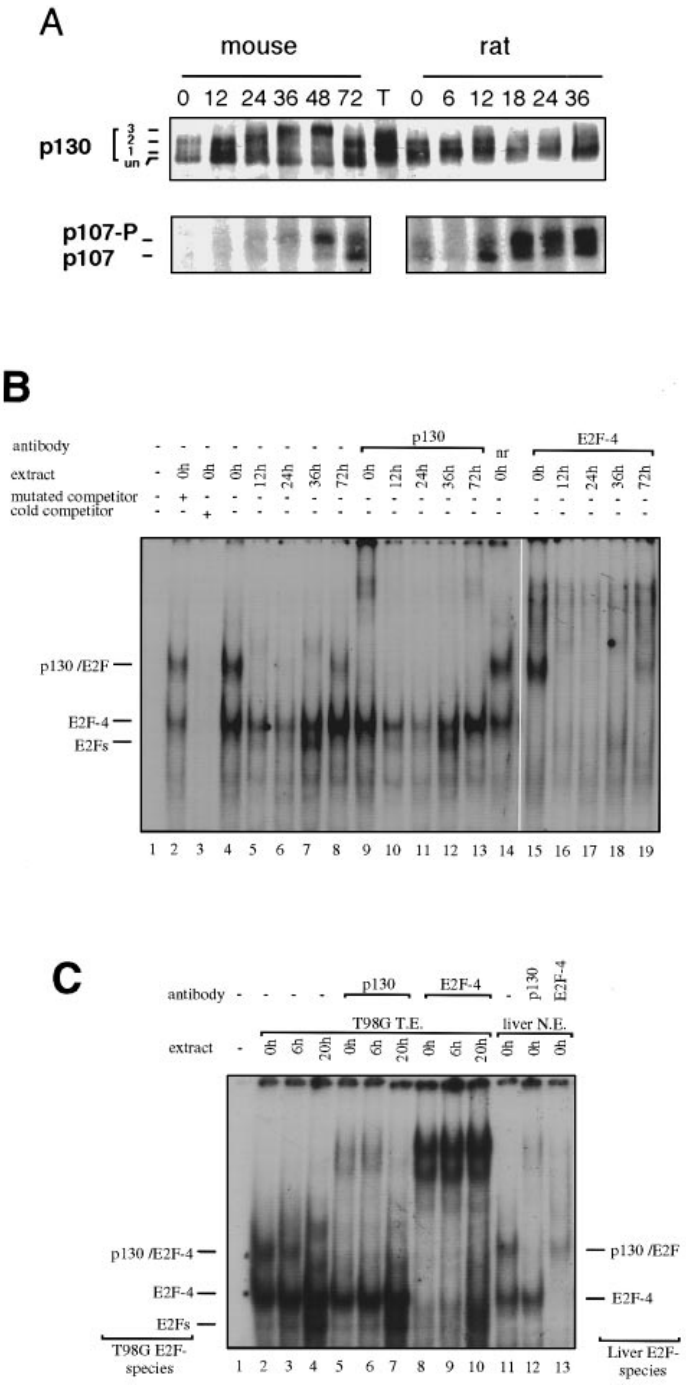

Figure 5 Changes *in vivo* of the phosphorylation status and protein levels of p130 and p107 in regenerating liver in mouse and rat

(**A**) Upper panel: 40 μg of protein extract obtained from regenerating mouse (lanes 1–6) and rat (lanes 8–13) livers at different time points after PH (see the Experimental section) was resolved in SDS/PAGE [6% (w/v) gel] and immunoblotted as in Figure 1 with specific antibodies. Asynchronously growing T98G glioblastoma cells were used as a control for the identification of the different phosphorylated forms of p130 (lane T). Lower panel: p107 patterns in samples obtained after PH were determined by immunoprecipitation followed by Western blotting with anti-p107 antibodies. Protein (300 μg) for each time point was immunoprecipitated with anti-p107 antibodies. Immunoprecipitates were resolved by SDS/PAGE [6% (w/v) gel] and immunoblotted with anti-p107 antibodies as in Figure 1. Time points after hepatectomy are indicated in hours at the top. (**B**, **C**) EMSAs were performed as described in the Experimental section. The time points, addition of competitor oligonucleotide and antibodies used for the supershifts are indicted at the top. E2F species are indicated. (**B**) E2F–DNA-binding activities during liver regeneration. (**C**) Comparison of E2F species from quiescent and proliferating T98G cells and mouse liver nuclei.

Regulation of pocket protein levels during models of cell proliferation *in vivo*

p130 and p107 undergo changes in protein levels and phosphorylation state in cultured quiescent cells and cells progressing through the cell cycle [16,17,31]. To ascertain whether a similar modulation of p130 and p107 proteins also takes place during cell cycle re-entry of cells differentiated *in vivo*, we analysed the p130 and p107 patterns during tissue regeneration *in vivo* after PH in the rat and mouse, and after acute arterial injury in the rat.

Rat and mouse models of liver regeneration after 70% PH

Rat and mouse liver regeneration after PH are two well-characterized models of cell proliferation *in vivo*. The decrease in liver mass resulting from surgical hepatectomy triggers the synchronized proliferation of hepatocytes in the remaining lobes, resulting in the restoration of liver mass and function. Entrance of hepatocytes to the cell cycle can be monitored by peaks of DNA synthesis after PH at approx. 24 h in the rat and 36 h in the mouse and by timed synthesis of cyclins and CDKs that results in the activation of cyclin/CDK holoenzymes [32–34]. Protein extracts obtained from the livers at different time points after PH were prepared and analysed by Western blotting. Both mouse and rat adult livers contained the unphosphorylated and the phosphorylated forms 1 and 2 of p130 (Figure 1, and Figure 5A, 0 h), which is the G_0 pattern consistent with the differentiated state of adult hepatocytes. As expected, PH caused the phosphorylation of p130 to form 3 (Figure 5A, 24–48 h in the mouse and 12–36 h in the rat) during periods before and simultaneous with the entrance of hepatocytes into the S phase [33,34]. However, p130 forms 1 and 2 did not disappear, nor did p130 total protein levels seem to diminish on G_1/S-phase progression, which is in contrast with previous results obtained with cultured cells. This result was expected because the entire population of hepatocytes does not enter the cell cycle during the first proliferative wave after PH; thus a residual proportion of hepatocytes will account for the presence of p130 forms 1 and 2. Moreover because most regenerating hepatocytes divide only once [35], cell cycle progression during liver regeneration seems to be similar to that in culture conditions *in vitro* described previously, in which cells progress through S and G_2/M phases in the absence of serum, in which case the next exit from mitosis leads to a direct entrance into G_0 [16]. In neither case does down-regulation of p130 form 3 occur in the S phase.

In contrast with p130, the analysis of the expression and phosphorylation status of p107 showed almost undetectable levels of p107 in adult liver (Figures 1 and 5A). Regeneration after PH resulted in an increase in p107 expression and in the appearance of hyperphosphorylated p107, correlated with the presence of p130 form 3, suggesting that similar G_1 cyclin/CDK holoenzymes target these pocket proteins co-ordinately. As observed in cells grown *in vitro*, p107 expression and post-translational modifications were observed mainly in cycling cells. p107 levels were again shown to be tightly regulated during a proliferative process *in vivo*; interestingly, this regulation seems to be independent of the state of phosphorylation of p107.

We also analysed E2F–DNA-binding activities in nuclear protein extracts of adult and regenerating mouse livers by EMSA. Adult liver nuclei contained two major E2F complexes (Figure 5B, lane 4). The fastest-migrating E2F complex contained E2F-4, whereas the slowest contained p130, as demonstrated by supershift of these complexes with anti-E2F-4 and anti-p130 antibodies respectively (Figure 5B; compare lane 4 with lanes 9 and 15). Marked changes in E2F–DNA-binding activities were detectable as early as 12 h after hepatectomy. The p130/E2F

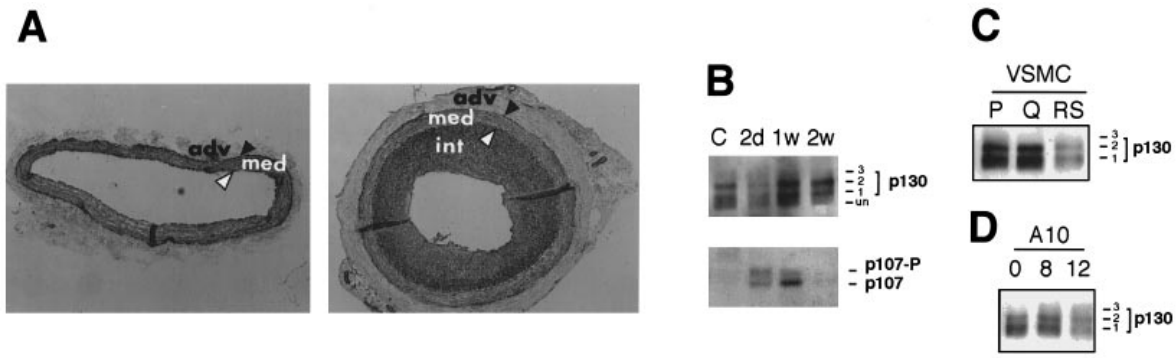

Figure 6 p130 expression in different models *in vivo* and *in vitro* of smooth-muscle cell cycle re-entry

(**A**) Smooth-muscle α-actin immunohistochemical staining of uninjured rat carotid artery (left panel) and 2 weeks after balloon angioplasty (right panel). In this model, injury-induced VSMC proliferation and migration results in intimal lesion formation within 2 weeks of angioplasty. Cross-sections of arteries were immunostained with mouse anti-(smooth-muscle α-actin) monoclonal antibody as described previously [21]. Black and white arrowheads point to the external and internal elastic laminae respectively. Abbreviations: adv, adventitia; med, media; int, intimal lesion. Magnification $\times 20$. (**B**) Protein lysate (40 μg) from control (C) and balloon-injured rat carotid arteries at different times (2 days and 1 and 2 weeks) after angioplasty was analysed by Western blotting with specific anti-p130 and anti-p107 antibodies as in Figure 1. Protein forms are indicated at the right. (**C**) Primary cultures of rat aorta VSMCs were maintained at subconfluence in growth medium [proliferating (P)], serum-starved for 3 days [quiescent (Q)] or serum-starved for 3 days and re-stimulated for 1 day with growth medium (RS). Protein extracts were analysed by Western blotting as in Figure 1 with anti-p130 antibodies. Protein forms are indicated at the right. (**D**) Quiescent rat aorta A10 cells were serum-starved (0) and re-stimulated with FBS (see the Experimental section). Cells were harvested at the indicated time points (in hours), and protein extracts were analysed by Western blotting as in Figure 1 with the use of specific anti-p130 antibodies. Protein forms are indicated at the right.

complex disappeared and the E2F-4 complex seemed to be down-regulated initially and up-regulated to maximal levels by 36 h, coinciding with the S phase (Figure 5B; compare lanes 5–7). A new E2F complex not containing E2F-4 was detected at that time and disappeared by 72 h, coinciding with the re-appearance of the p130/E2F species and cell cycle exit (Figure 5B; compare lanes 7 and 8). Other E2F complexes not containing p130 were detected between 12 and 36 h. Anti-p107 antibodies did not supershift any of these complexes, suggesting that E2F/p107 complexes are absent or scarce. Interestingly, antibodies against E2F-4 supershifted most E2F complexes but did not supershift most of the E2F complex containing p130 in quiescent liver nuclei (Figure 5B; compare lane 4 with lanes 9 and 15, and lane 8 with lanes 13 and 19). This is in contrast with similar experiments performed with quiescent human T98G cells. Two major E2F complexes were detected in serum-starved T98G cells, co-migrating with those detected in nuclei from adult liver (Figure 5C; compare lanes 2 and 11). However, whereas the slowest E2F complex detected in quiescent T98G cells contained both p130 and E2F-4 (Figure 5C; compare lanes 2 and 3 with lanes 5 and 6 and lanes 8 and 9), the co-migrating complex in liver nuclei was not supershifted by the anti-E2F-4 antibody (Figure 5C; compare lanes 11–13). Thus these experiments seem to indicate that p130 associates with an E2F family member other than E2F-4 in mouse adult liver.

Rat acute arterial injury

During homoeostasis, VSMCs display a differentiated phenotype and are quiescent. However, in contrast with skeletal and cardiac myocytes, VSMCs can re-enter the cell cycle after appropriate stimuli [36]. The modulation of the expression and phosphorylation of p130 and p107 was examined after balloon angioplasty in the rat carotid artery. In this model, balloon denudation triggers a rapid proliferative response of VSMCs in the media, followed by a second proliferative wave within the intimal lesion [37,38], which leads to intimal lesion formation (Figure 6A). It has been shown previously that the thymidine index in the media peaks approx. 2 days after angioplasty [26], coincident with the induction of CDK2 and its regulatory subunits, cyclins E and A [21]. Protein lysates were prepared at different time points after angioplasty and examined by Western blot analysis. As shown in Figure 6(B), control adult rat carotid arteries exhibited the pattern of p130 forms characteristic of quiescent cells: unphosphorylated and phosphorylated p130 forms 1 and 2. These forms were markedly down-regulated 2 days after angioplasty and low levels of p130 form 3 were detectable at this time point. As occurred after PH (see above), low levels of p130 forms 1 and 2 were also observed, coinciding with VSMC proliferation *in vivo*. This could be explained by the presence of non-proliferating cells in the samples, as occurred after PH, owing to poor cell cycle synchrony because of the spatial and temporal dependence in the activation of the different smooth-muscle cell layers. At 1 week after angioplasty, the levels of p130 forms 1 and 2 returned to control levels. Nevertheless the most significant finding was again the abrupt up-regulation of p107 levels that were seen during the proliferative activation, in a manner similar to the effects induced on p107 after PH (Figures 5B and 6B). The increase in p107 levels also seemed to occur independently of p107 hyperphosphorylation. These findings are therefore consistent with p107's expression and phosphorylation being restricted to cycling VSMCs.

Because the modulation of p130 was less apparent in the vascular regeneration model, probably owing to the heterogeneous synchrony in proliferation of the different smooth-muscle cell layers, we analysed p130 by Western blotting during the synchronous proliferation of primary rat aortic VSMCs. These cells display a differentiated, quiescent phenotype under serum starvation and can re-enter the cell cycle after appropriate stimuli. As shown in Figure 6(C), asynchronously growing primary VSMCs showed low levels of hyperphosphorylated p130 form 3 together with higher levels of forms 1 and 2; this could be explained by the fact that a portion of the cells in these cultures might not have been proliferating, owing to contact inhibition. When these cells were made quiescent, p130 form 3 consistently disappeared, coinciding with a slight accumulation of p130 forms

1 and 2. Re-entry of these cells into the cell cycle resulted in the down-regulation of p130 forms 1 and 2 and the reappearance of p130 form 3, although at very low levels; this could be explained by the fact that a proportion of the cell population did not re-enter the cell cycle. It is also conceivable that p130 form 3 is found in vascular aortic cells in such low levels because this form is extremely unstable in these cells and is therefore degraded very early after phosphorylation in mid-G_1. Finally, the modulation of p130 was also analysed in serum-starved and re-stimulated rat aorta A10 smooth-muscle cells (Figure 6D). p130 form 3 was clearly detected as cells re-entered G_1 from G_0, whereas the levels of p130 forms 1 and 2 decreased. The clear detection of phosphorylation of p130 to form 3 is consistent with a larger number of cells progressing synchronously through G_1 in this culture model *in vitro* (see above).

DISCUSSION

In the present study, protein levels and the phosphorylation of pocket proteins are shown to be tightly and differently regulated in various models of cell proliferation and differentiation. Three main conclusions are derived from the present study. First, distinct changes in pocket protein levels are shown to occur in a conserved fashion in different models, and this differential regulation parallels some of the changes in the composition of E2F complexes. Secondly, phosphorylation events and the accumulation of p130 characteristic of departure from the cell cycle [16] are shown here to be conserved when transit to G_0 also involves terminal differentiation. Interestingly, whereas p130 phosphorylation status seems to be coupled to the levels of p130 protein, the phosphorylation status of pRB and p107 does not. Thirdly, p130 and p107 levels and phosphorylation status are regulated *in vivo* as in cultured cells. The modulation of p130 phosphorylation status is correlated with changes in E2F activities *in vivo*.

Differential regulation of pocket protein levels

The differential regulation of pocket protein levels shown here might have direct implications for our understanding of the regulation of the repressing activity of pocket proteins on E2F-dependent transcription, and in particular the repression of E2F-4 by p130 and p107. The up-regulation of p130 and the down-regulation of p107 levels during differentiation shown here are a plausible explanation of the fact that the differentiation *in vitro* of some cell types, including muscle cells, involves a change from p107/E2F-4 complexes in proliferating cells to p130/E2F-4 complexes in differentiated cells [11–15]. Similarly, changes in p130 and p107 levels observed previously during the cell cycle progression of cell lines *in vitro* [16,17,31] are reproduced here in models of tissue regeneration *in vivo* (Figures 5 and 6). This might also explain why p130/E2F-4 complexes are the only E2F complexes found in a number of quiescent cells, and why progression through the G_1 phase involves a complete shift of E2F-4 from p130 to p107 and the pRB complexes [4,5,9,10]. Therefore, although cyclin/CDK phosphorylation regulates the interaction of E2F-4 with p130 and p107, it is not sufficient to explain the changes in the composition of E2F-4 complexes during the processes studied. Instead, the regulation of p130 and p107 levels is a probable mechanism of regulation of the composition of E2F-4 complexes in particular cellular stages.

The mechanisms underlying the regulation of p130 and p107 levels are clearly distinct. Present and previous results suggest that specific phosphorylation events of p130 affect the stability of the protein [1,2]. First, phosphorylation of p130 to the cell cycle exit-specific forms 1 and 2 is correlated with the accumulation of p130 protein in the cell, but cyclin/CDK phosphorylation to form 3 in mid-G_1 phase is followed by marked down-regulation of the p130 protein [6,16,17]. Secondly, labelling experiments *in vivo* with either [^{35}S]methionine or [^{32}P]P_i showed that radioactivity is poorly incorporated in p130 forms 1 and 2 of quiescent cells but is much more efficiently incorporated in p130 form 3 of proliferating cells [14,17]. Interestingly, p130 form 2 was not labelled in these experiments. Therefore both the synthesis and the phosphorylation turnover of p130 forms 1 and 2 are much slower than the turnover of p130 form 3. Consistent with this, it is conceivable that the phosphorylation of p130 to forms 1 and 2 results in the stabilization of p130, therefore requiring a slower turnover to maintain the high levels of forms 1 and 2 present in quiescent cells. This model is also consistent with the low rate of synthesis of p130 detected in differentiated compared with proliferating C2C12 cells [13] and with a recent report showing that steady-state levels of p130 transcripts are not regulated during differentiation [39]. This possibility is particularly interesting because it has been shown that p130 stabilizes E2F-4, protecting it from degradation by the ubiquitin proteasome machinery [40]. Thus the stabilization of p130 by cell cycle exit-specific phosphorylation would in turn result in the accumulation of p130/E2F-4 complexes to repress the transcription of certain genes during G_0 and early G_1 [6,7,41–43].

p107 is hyperphosphorylated by cyclin/CDKs to a form with an electrophoretic mobility slower than the hypophosphorylated form [31]. In contrast with p130, the state of phosphorylation of p107 seems to be independent of changes in its protein levels, as seen in the present study. Moreover it does not undergo the cell cycle exit-induced phosphorylation characteristic of p130. Interestingly, the p107 gene promoter has been shown to contain two E2F sites that can drive the transcription of a reporter gene fused to this promoter, and this promoter can be repressed by pocket proteins [44]. This result suggests that transcription of p107 is, at least in part, under E2F control and probably regulated during the cell cycle. It is thus tempting to speculate not only that the disruption of p130/E2F-4 complexes in mid-G_1 results in the transcription of E2F-1 [7], but that either active free E2F-4 or the newly synthesized E2F-1 activates the transcription of p107. Further experiments are required to test this possibility.

Apart from the differential regulation of pocket protein levels, two points regarding the regulation of p130 during both cell differentiation and cell cycle re-entry *in vivo* deserve further discussion.

Regulation of p130 during differentiation

The behaviour of p130 forms during differentiation is in striking contrast with the changes observed for the p107 protein, and all protein patterns are consistent with the profiles of these proteins in mouse tissues (see above). The modulation of the phosphorylation and levels of p130 during skeletal muscle differentiation as well as during granulocytic differentiation of 32Dcl3 cells is consistent with our previous analysis of p130 regulation in cells exiting from the cell cycle to quiescence [16]. p130 form 3 is clearly detectable in proliferating C2C12 and L6 myoblasts, and in the initial proliferative phase induced by G-CSF in 32Dcl3 cells (Figures 3 and 4). In both differentiation models, the accumulation of p130 forms 1 and 2 (which are phosphorylated forms) correlates with growth arrest and the initiation of terminal differentiation. High levels of these forms are maintained in terminally differentiated myotubes, consistent with a role for p130 in the maintenance of this differentiated state. Interestingly, it has been shown that the E2F complexes from quiescent and differentiated cells, which contain p130 as a major associated

pRB-related protein, can be distinguished [11,13,15]: whereas in differentiated C2 cells there is a single E2F complex that contains p130, in the C2 differentiation-defective derived cell line NFB, there are various E2F activities [11]. A comparison of the protein levels and phosphorylation status of p130 in differentiated C2C12 cells and quiescent NFB cells did not reveal any marked difference. However, we cannot exclude the possibility that although the p130 phosphorylated forms of quiescent undifferentiated NFB and differentiated C2C12 muscle cells co-migrate, they might be phosphorylated at different sites. A definitive answer will require the identification of the phosphorylation sites on p130 after exit from cell cycle.

Modulation of the phosphorylation status of p130 in models *in vivo* of cellular proliferation

The extremely low levels of p130 form 3 in mouse tissues prompted us to analyse whether its absence was correlated with the fact that most of the cells in these tissues were in G_0. Phosphorylation of p130 to form 3 in livers after PH occurred at a time consistent with hepatic cells being in G_1, before the peak of DNA synthesis and coinciding with the expression and activation of cyclin D1 [25]. Therefore, although the patterns of expression of G_1 cyclins and CDKs might vary significantly between different mammalian species during hepatic regeneration [25], the phosphorylation of p130 and p107 seems to be similarly regulated during both liver regeneration and cells grown in culture, and our results are consistent with similar cyclin/CDK holoenzymes targeting pocket proteins co-ordinately. In addition, the disruption and reappearance of p130/E2F complexes during hepatic proliferation and differentiation *in vivo* is consistent with changes on the phosphorylation status of p130. Although E2F complexes have been analysed occasionally in adult mammalian tissues [13,45], to the best of our knowledge this is the first report describing the regulation of p130/E2F complexes in a proliferative process *in vivo*.

By using the rat carotid model of angioplasty it has been shown the temporal and spatial correlation between injury-induced VSMC proliferation and the expression of CDK2 and cyclins A and E [21]. Acute arterial injury results in the down-regulation of p130 within 8 h (results not shown) and several days after injury; however, p130 form 3 is hardly detectable at any time. One possibility is that p130 form 3 might be extremely unstable in proliferating VSMCs and is therefore degraded very early after phosphorylation in mid-G_1, which is in agreement with the down-regulation of p130 form 3 from mid-G_1 to mitosis [16,17] and with the low levels of p130 in some cell lines growing exponentially [6]. In addition, different waves of proliferation in the media and intima after angioplasty [26] might partly mask the presence of p130 form 3 owing to the high levels of p130 forms 1 and 2 in quiescent cells. Serum re-stimulation of primary rat VSMCs and rat aorta A10 cells (Figures 6C and 6D) resulted in detectable levels of p130 form 3. As mentioned above, the regulation of p107 levels is in striking contrast with that of p130. The opposite regulation of these two proteins *in vivo* further highlights their distinguishable functions.

As regards p130, the results reported here demonstrate that its regulation is highly conserved during the mammalian cell cycle, as well as the exit from the cell cycle to differentiation, both *in vivo* and *in vitro*. Phosphorylation of p130 during the exit from the cell cycle might have a crucial role in regulating the accumulation of p130, thus allowing the accumulation of p130/E2F transcriptional repressors of growth-regulatory genes. Interestingly, the fact that cell cycle exit-induced phosphorylation of p130 to forms 1 and 2 is conserved after cell differentiation indicates that the cell cycle exit-induced kinase(s) targeting p130 at this stage are active in differentiating cells.

We thank John Gibas for performing the flow cytometric analysis, Michelle Akiko for technical assistance on the characterization of 32Dcl3 cells, Cory Ahonen and Brenda Rieland for excellent technical assistance with mouse and rat liver hepatectomies, Kevin Krasinski for excellent technical assistance with the balloon angioplasty procedure, Matilde Parreño for critical reading of the manuscript, and Jonathan Pines and Andrew Koff for antibodies. J.G. was initially supported by a CIRIT fellowship (Generalitat de Catalunya), J.G. and X.M. were supported by a fellowship from Dirección General de Investigación Científica y Técnica (Ministerio de Educación y Ciencia, Spain), A.L. was supported by a Lady Tata fellowship, and J.H.A. was supported by a grant from the American Liver Foundation. This work was supported by an Institutional ACS grant no. ACS IRG-204, a Wendy Will Case Cancer Fund grant and a grant from the National Institute of General Medical Sciences, NIH (GM54894) (X.G.).

REFERENCES

1 Mayol, X. and Graña, X. (1998) Frontiers Biosci. **3**, 11–24
2 Mayol, X. and Graña, X. (1997) in Progress in Cell Cycle Research, vol. 3 (Meijier, L. G. S. and Philippe, M., eds.), pp. 157–169, Plenum Press, New York
3 Graña, X. and Reddy, E. P. (1995) Oncogene **11**, 211–219
4 Ikeda, M., Jakoi, L. and Nevins, J. R. (1996) Proc. Natl. Acad. Sci. U.S.A. **93**, 3215–3220
5 Cobrinik, D., Whyte, P., Peeper, D. S., Jacks, T. and Weinberg, R. A. (1993) Genes Dev. **7**, 2392–2404
6 Smith, E. J., Leone, G., Degregori, J., Jakoi, L. and Nevins, J. R. (1996) Mol. Cell. Biol. **16**, 6965–6976
7 Johnson, D. G. (1995) Oncogene **11**, 1685–1692
8 Wolf, D. A., Hermeking, H., Albert, T., Herzinger, T., Kind, P. and Eick, D. (1995) Oncogene **10**, 2067–2078
9 Vairo, G., Livingston, D. M. and Ginsberg, D. (1995) Genes Dev. **9**, 869–881
10 Moberg, K., Starz, M. A. and Lees, J. A. (1996) Mol. Cell. Biol. **16**, 1436–1449
11 Shin, E. K., Shin, A., Paulding, C., Schaffhausen, B. and Yee, A. S. (1995) Mol. Cell. Biol. **15**, 2252–2262
12 Halevy, O., Novitch, B. G., Spicer, D. B., Skapek, S. X., Rhee, J., Hannon, G. J., Beach, D. and Lassar, A. B. (1995) Science **267**, 1018–1021
13 Corbeil, H. B., Whyte, P. and Branton, P. E. (1995) Oncogene **11**, 909–920
14 Kiess, M., Gill, R. M. and Hamel, P. A. (1995) Cell Growth Differ. **6**, 1287–1298
15 Jiang, H. P., Lin, J., Young, S. M., Goldstein, N. I., Waxman, S., Davila, V., Chellappan, S. P. and Fisher, P. B. (1995) Oncogene **11**, 1179–1189
16 Mayol, X., Garriga, J. and Graña, X. (1996) Oncogene **13**, 237–246
17 Mayol, X., Garriga, J. and Graña, X. (1995) Oncogene **11**, 801–808
18 Peterson, C. A., Gordon, H., Hall, Z. W., Paterson, B. M. and Blau, H. M. (1990) Cell **62**, 493–502
19 Patel, G., Kreider, B., Rovera, G. and Reddy, E. P. (1993) Mol. Cell. Biol. **13**, 2269–2276
20 Pickering, J. G., Weir, L., Rosenfield, K., Stetz, J., Jekanowski, J. and Isner, J. M. (1992) J. Am. Coll. Cardiol. **20**, 1430–1439
21 Wei, G. L., Krasinski, K., Kearney, M., Isner, J. M., Walsh, K. and Andres, V. (1997) Circ. Res. **80**, 418–426
22 Schreiber, E., Matthias, P., Muller, M. M. and Schaffner, W. (1989) Nucleic Acids Res. **17**, 6419
23 Fattaey, A. R., Harlow, E. and Helin, K. (1993) Mol. Cell. Biol. **13**, 7267–7277
24 Hattori, M., Tugores, A., Veloz, L., Karin, M. and Brenner, D. A. (1990) DNA Cell. Biol. **9**, 777–781
25 Albrecht, J. H., Hu, M. Y. and Cerra, F. B. (1995) Biochem. Biophys. Res. Commun. **209**, 648–655
26 Clowes, A. W., Reidy, M. A. and Clowes, M. M. (1983) Lab. Invest. **49**, 327–333
27 Garriga, J., Mayol, X. and Graña, X. (1996) Biochem. J. **319**, 293–298
28 Cleaver, J. (1967) in Frontiers in Biology, vol. 6 (Neuberger, A. and Tatum, E., eds.), pp. 184–233, North-Holland, Amsterdam/John Wiley, New York
29 Andres, V. and Walsh, K. (1996) J. Cell Biol. **132**, 657–666
30 Valtieri, M., Tweardy, D. J., Caracciolo, D., Johnson, K., Mavilio, F., Altmann, S., Santoli, D. and Rovera, G. (1987) J. Immunol. **138**, 3829–3835
31 Beijersbergen, R. L., Carlee, L., Kerkhoven, R. M. and Bernards, R. (1995) Genes Dev. **9**, 1340–1353
32 Albrecht, J., Poon, R. Y. C., Ahonen, C., Rieland, B., Deng, C. and Crary, G. (1998) Oncogene **16**, in the press
33 Albrecht, J. H., Hoffman, J. S., Kren, B. T. and Steer, C. J. (1994) FEBS Lett. **347**, 157–162
34 Steer, C. J. (1995) FASEB J. **9**, 1396–1400
35 Fabrikant, J. I. (1968) J. Cell Biol. **36**, 551–565

36 Owens, G. K. (1995) Physiol. Rev. **75**, 487–517
37 Schwartz, S. M., deBlois, D. and O'Brien, E. R. (1995) Circ. Res. **77**, 445–465
38 Schwartz, R. S. (1994) Lab. Invest. **71**, 789–791
39 Richon, V. M., Lyle, R. E. and McGehee, R. E. (1997) J. Biol. Chem. **272**, 10117–10124
40 Hateboer, G., Kerkhoven, R. M., Shvarts, A., Bernards, R. and Beijersbergen, R. L. (1996) Genes Dev. **10**, 2960–2970
41 Tommasi, S. and Pfeifer, G. P. (1995) Mol. Cell. Biol. **15**, 6901–6913
42 Lam, E. W. and Watson, R. J. (1993) EMBO J. **12**, 2705–2713
43 Ohtani, K., Degregori, J., Leone, G., Herendeen, D. R., Kelly, T. J. and Nevins, J. R. (1996) Mol. Cell. Biol. **16**, 6977–6984
44 Zhu, L., Zhu, L., Xie, E. and Chang, L. S. (1995) Mol. Cell. Biol. **15**, 3552–3562
45 Williams, C. D., Linch, D. C., Sorensen, T. S., Lathangue, N. B. and Thomas, N. S. B. (1997) Br. J. Haematol. **96**, 688–696

Received 11 March 1998; accepted 28 April 1998